Supplementary Appendix to: Probabilistic Forecasting of Bubbles and Flash Crashes.

Anurag Banerjee
Durham Business School

Guillaume Chevillon
ESSEC Business School *

Marie Kratz
ESSEC Business School, CREAR

September 12, 2018

1 Simulations of Predictive Probabilities

To study the patterns generated by predictive probabilities, we simulate using 10^5 Monte Carlo replications the values of $\pi_{t,h}(\gamma)$ defined in (10) for $\gamma = 1.05$ and $\alpha = .8$. We consider $(\phi, \lambda) \in \{-1, 0, 1\} \times \{0, 5, 1, 2, 3\}$, and $h \in \{1, 6, 24\}$. In Figure S.1, we report simulated $\pi_{t,h}(\gamma)$ for a large sample size $T = 1000$ where $900 \leq t \leq 1000$. Figure S.2 records similar simulations for a smaller sample size $T = 200$ and we let $100 \leq t \leq 200$.

When $\phi = -1$ and for the range of (λ, h) considered, with $\gamma > 1$, both figures report probabilities that hover below .50 and that decrease with h since the latter impacts positively the variance of conditional forecasts. Probabilities reported in Figure S.1 hardly vary with t, which shows that they are obtained from the ergodic distributions of the weakly stationary process. This is not the case when γ is time varying (e.g. a risk free rate) or for the smaller sample size reported in Figure S.2 where predictive probabilities tend to decrease as t increases.

For positive values of ϕ, the probabilities process reported in Figure S.1 tend to be more dispersed as of function λ and get closer to 0.5 as λ and h increases. They are also more stable as a function of t for larger values of λ. In the relatively large sample considered in the figure, the predictive probabilities are always below .5 except when $\phi = 1$ and $h = 24$. By contrast, in the smaller sample size recorded in Figure S.2, $\pi_{t,h}(\gamma) > .5$ for smaller values of

*Corresponding author. Email: chevillon@essec.edu; Address: ESSEC Business School, Avenue B. Hirsch, 95021 Cergy-Pontoise, FRANCE.

h when $\phi > 0$. This reflects the larger $\mathsf{E}\left(\rho_t^2\right)$ induced by the smaller T. Notice also that for so small a sample, the probabilities exhibit trending patterns as function of t.

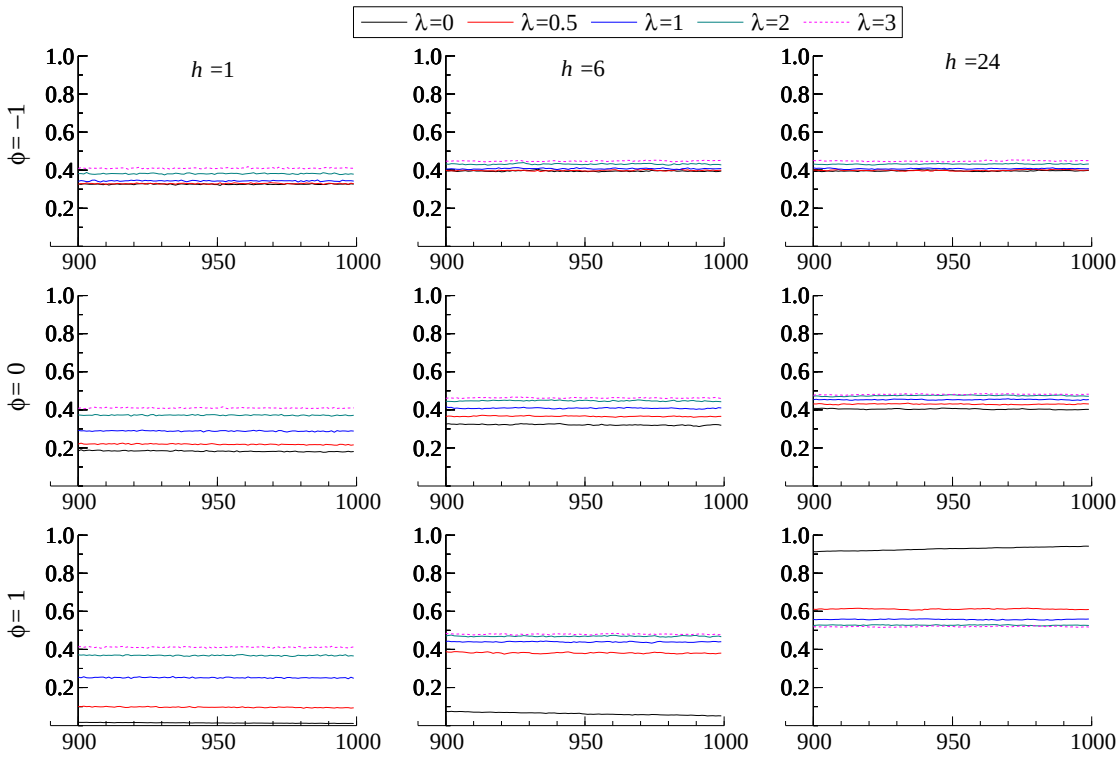

Figure S.1: The figure presents records simulated probabilities $\pi_{t,h}(\gamma)$ for $\gamma = 1.05$ and $900 \leq t \leq 1000$ and $\alpha = .8$. Each row records a different value of $\phi \in \{-1, 0, 1\}$, and each column a value of the horizon $h \in \{1, 6, 24\}$; the graphs record different values of $\lambda \in \{0, .5, 1, 2, 3\}$. The number of Monte Carlo replications is 5×10^4.

2 Additional Empirical Applications

Figure S.3 considers the logarithm of the S&P 500 index since the early 1950s with $\gamma = 1.004$, which corresponds to an annual rate of growth of 5% – approximately the long run nominal growth of the economy. Throughout the sample, $\widehat{\pi}_{t,h}^{\min}(\gamma) < 0.5$ yet close to it (a random walk yields zero probability of a bubble according to our local-asymptotic definition but $\Pr(y_{t+h}/y_t > 1|\mathcal{I}_t) = 0.5$ for t finite and $h \geq 1$), and $\widehat{\pi}_{t,h}^{\max}$ is strictly less than unity over the first two thirds of the sample, with $\widehat{\pi}_{t,h}^{med}(\gamma)$ close to 0.66. $\widehat{\pi}_{t,h}^{\max}(\gamma)$ increases over the sample to stabilize at 1, reflecting the growth of the data which does not preclude the possibility of explosive growth.

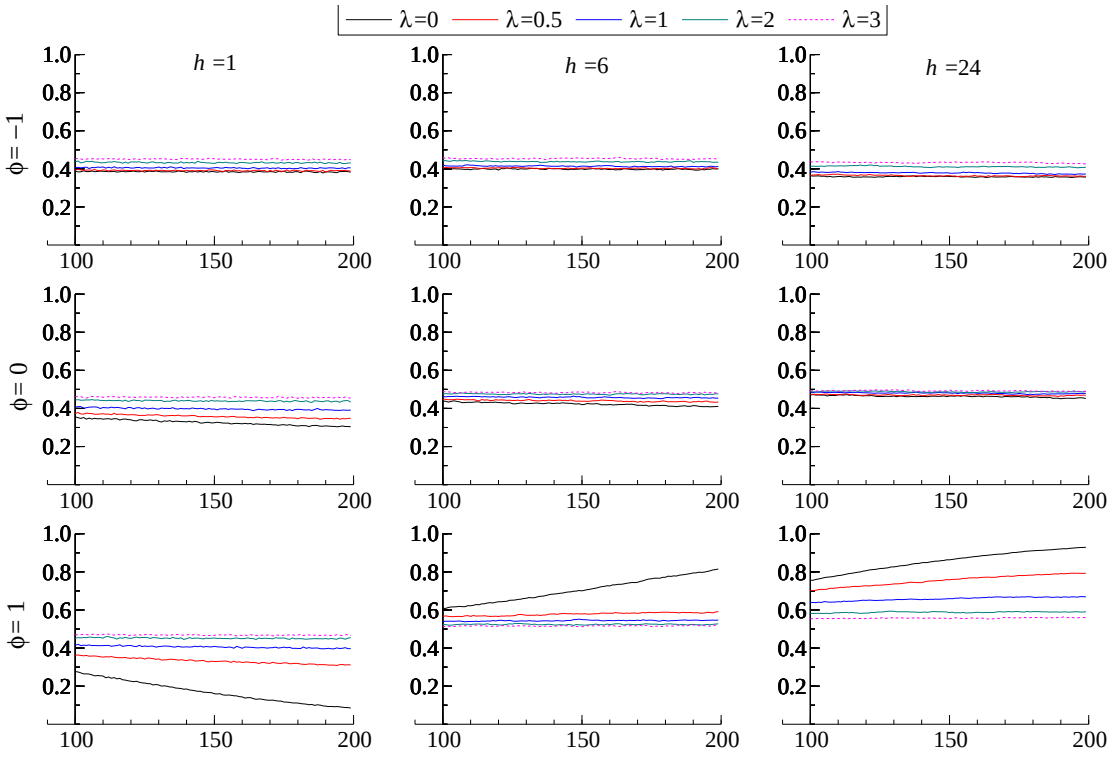

Figure S.2: The figure presents records simulated probabilities $\pi_{t,h}(\gamma)$ for $\gamma = 1.05$, $100 \leq t \leq 200$ and $\alpha = .8$. Each row records a different value of $\phi \in \{-1, 0, 1\}$, and each column a value of the horizon $h \in \{1, 6, 24\}$; the graphs record different values of $\lambda \in \{0, .5, 1, 2, 3\}$. The number of Monte Carlo replications is 5×10^4.

Comparable results are reported in Figure S.4 for the logarithm of the long term interest rates since the early 1960s with $\gamma = 1$. We notice the stability of the estimated probabilities. The main difference with the previous figure is that since the interest rate reverts towards the end of the sample to the values observed at the beginning, minimum and maximum probabilities shift downwards, with $\widehat{\pi}_{t,h}^{\max}(\gamma) < 1$, towards the end of the sample, which widens the range of predictive probabilities.

3 Technical Proofs

We collect here the proofs that R_t and R_t^* can be neglected in the expressions where they appear in the proofs above.

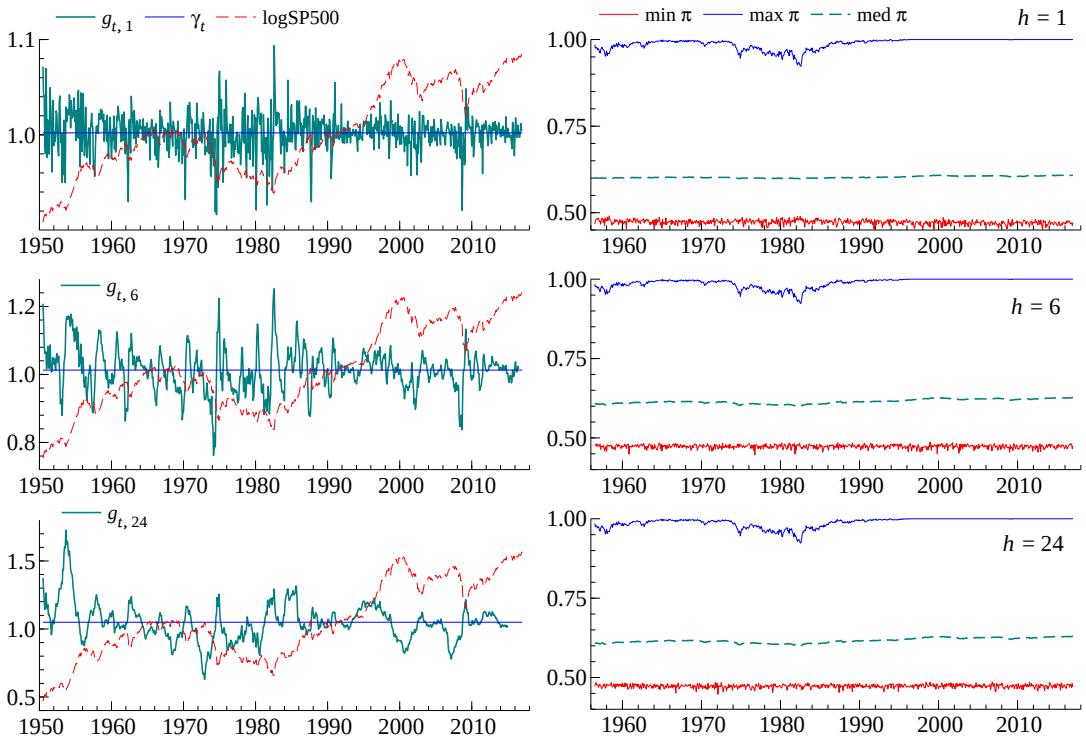

Figure S.3: Predictive probabilities for the logarithm of the monthly S&P 500 stock index. The left column reports the actual series as well as the growth $g_{t,h} = y_{t+h}/y_t$ for horizons $h = 1, 6$ and 24 in, respectively, the top, middle and bottom rows. The log price data are scaled to match the mean and range of $g_{t,h}$. The benchmark γ_t for computing probabilities is set to 1.004 for all horizons. The column on the right reports probabilities $\widehat{\pi}_{t,h}^{\min}(\gamma_t)$, $\widehat{\pi}_{t,h}^{\max}(\gamma_t)$ and $\widehat{\pi}_{t,h}^{med}(\gamma_t)$. Minimum and maximum are computed over the set of parameters which are not rejected at a nominal size of 0.10.

3.1 Case of R_t

We show here that the residual $R_{\lfloor \kappa_T \rfloor}$ appearing in S_{1T}, expression (25) is asymptotically negligible in probability with respect to the other terms.

Writing $R_t = R_{1t} - 2R_{2t}$ with

$$R_{1t} = \sum_{k=1}^{t} \left[\sum_{i=k+1}^{t} \exp\left(\frac{\phi}{T^{\alpha}} (k-i) - \frac{\lambda}{T^{\alpha/2}} (U_k - U_i) \right) \eta_i \right]^2$$

$$R_{2t} = \left(\sum_{i=1}^{t} \exp\left(-\frac{\phi}{T^{\alpha}} i - \frac{\lambda}{T^{\alpha/2}} U_i \right) \eta_i \right) \times \sum_{k=1}^{t} \sum_{i=k+1}^{t} \exp\left(\frac{\phi}{T^{\alpha}} (2k-i) + \frac{\lambda}{T^{\alpha/2}} (2U_k - U_i) \right) \eta_i$$

$$\equiv \left(\sum_{i=1}^{t} \exp\left(-\frac{\phi}{T^{\alpha}} i - \frac{\lambda}{T^{\alpha/2}} U_i \right) \eta_i \right) \times \overline{R}_{2t}.$$

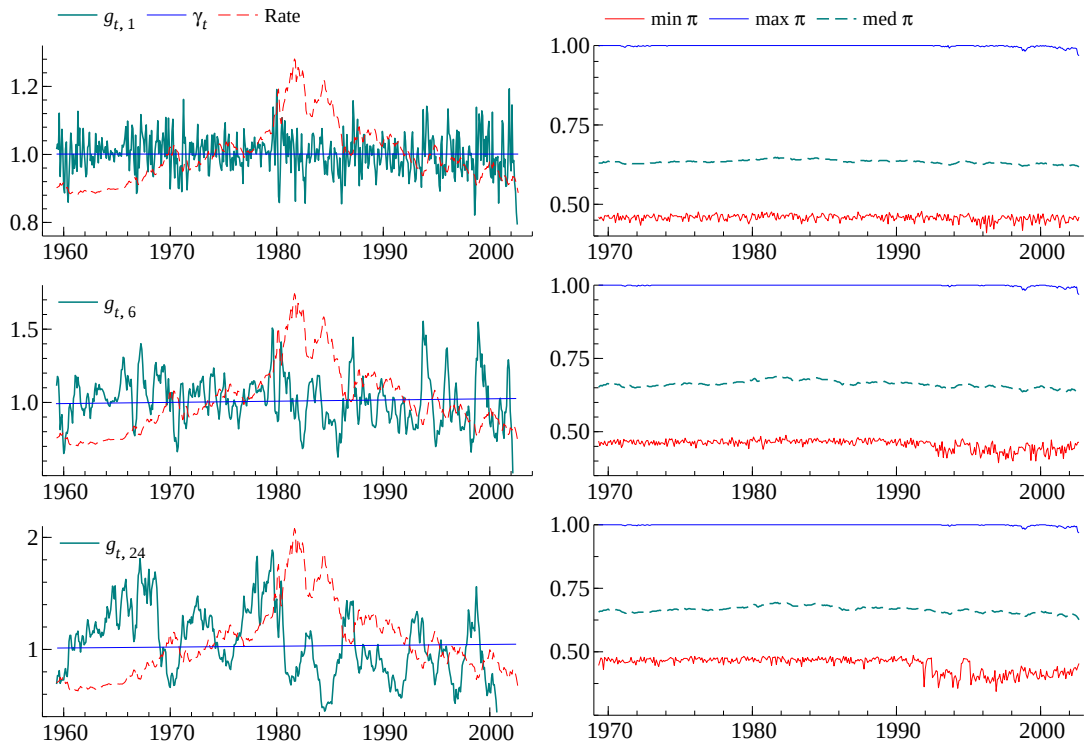

Figure S.4: Predictive probabilities for the U.S. monthly long run interest rate. The left column reports the actual series as well as the growth $g_{t,h} = y_{t+h}/y_t$ for horizons $h = 1, 6$ and 24 in, respectively, the top, middle and bottom rows. The interest rate data are scaled to match the mean and range of $g_{t,h}$. The benchmark γ_t for computing probabilities is set to 1 for all horizons. The column on the right reports probabilities $\widehat{\pi}_{t,h}^{\min}(\gamma_t)$, $\widehat{\pi}_{t,h}^{\max}(\gamma_t)$ and $\widehat{\pi}_{t,h}^{med}(\gamma_t)$. Minimum and maximum are computed over the set of parameters which are not rejected at a nominal size of 0.10.

First,

$$T^{-2\alpha}\ \psi_{\lfloor T^{1-\alpha}\rfloor}^{-1}\varphi_{\lfloor T^{1-\alpha}\rfloor}^{-2}R_{1\lfloor\kappa_T\rfloor} = \psi_{\lfloor T^{1-\alpha}\rfloor}^{-1}\int_0^{\lfloor T^{1-\alpha}\rfloor}\left(\sigma_\eta\varphi_{\lfloor T^{1-\alpha}\rfloor}^{-1}\int_r^{\lfloor T^{1-\alpha}\rfloor}e^{\phi(r-s)+\lambda(W_r-W_s)}dB_s\right)^2 dr+o_p(1)$$

uniformly, and since we also have

$$\begin{aligned}\mathsf{E}\left(\int_r^{\lfloor T^{1-\alpha}\rfloor}e^{\phi(r-s)-\lambda(W_r-W_s)}dB_s\right)^2 &= \int_r^{\lfloor T^{1-\alpha}\rfloor}e^{2\left(\phi+\lambda^2\right)(r-s)}ds\\ &= \frac{1-e^{-2\left(\phi+\lambda^2\right)\left(\lfloor T^{1-\alpha}\rfloor-r\right)}}{2\left(\phi+\lambda^2\right)} = O(1)\end{aligned}$$

uniformly in $r \leq T^{1-\alpha}$, we obtain

$$T^{-2\alpha}\psi^{-1}_{\lfloor T^{1-\alpha}\rfloor}\varphi^{-2}_{\lfloor T^{1-\alpha}\rfloor}R_{1\lfloor \kappa_T\rfloor} = O_p(1) \times O\left(\psi^{-1}_{\lfloor T^{1-\alpha}\rfloor}\int_0^{\lfloor T^{1-\alpha}\rfloor} dr\right) = O_p\left(\lfloor T^{1-\alpha}\rfloor\, \psi^{-1}_{\lfloor T^{1-\alpha}\rfloor}\right).$$

Next, we have $T^{-\alpha}\psi^{-1}_{\lfloor T^{1-\alpha}\rfloor}\overline{R}_{2\lfloor \kappa_T\rfloor} = O_p\left(\lfloor T^{1-\alpha}\rfloor\, \psi^{-1}_{\lfloor T^{1-\alpha}\rfloor}\right)$, so it follows that

$$T^{-2\alpha}\psi^{-1}_{\lfloor T^{1-\alpha}\rfloor}\varphi^{-2}_{\lfloor T^{1-\alpha}\rfloor}R_{2\lfloor \kappa_T\rfloor} = O_p\left(T^{1-3/2\alpha}\psi^{-1}_{\lfloor T^{1-\alpha}\rfloor}\varphi^{-1}_{\lfloor T^{1-\alpha}\rfloor}\right),$$

hence the result concerning $R_{\lfloor \kappa_T\rfloor}$.

3.2 Case of R_t^*

We check that the term in R_t^* could indeed be neglected in expression (32). It is enough to notice that R_t^* can be expressed as

$$\begin{aligned} R_t^* = & T^{\alpha/2}\sum_{t=0}^{T-1}\exp\left(\frac{2\phi}{T^\alpha}t + \frac{2\lambda}{T^{\alpha/2}}U_t\right)\left[\sum_{i=1}^{t}\exp\left(-\frac{\phi}{T^\alpha}i - \frac{\lambda}{T^{\alpha/2}}U_i\right)\eta_i\right]^2 \Delta U_{t+1}^\rho \\ & - T^{\alpha/2}\left(\sum_{k=1}^{T-1}\exp\left(\frac{2\phi}{T^\alpha}k + \frac{2\lambda}{T^{\alpha/2}}U_k\right)\Delta U_{k+1}^\rho\right)\left[\sum_{i=1}^{T}\exp\left(-\frac{\phi}{T^\alpha}i - \frac{\lambda}{T^{\alpha/2}}U_i\right)\eta_i\right]^2 \\ \equiv & R_{1t}^* - 2R_{2t}^*, \end{aligned}$$

with $R_{1t}^* \equiv T^{\alpha/2}\sum_{k=1}^{t}\left[\sum_{i=k+1}^{t}\exp\left(\frac{\phi}{T^\alpha}(k-i) - \frac{\lambda}{T^{\alpha/2}}(U_k - U_i)\right)\eta_i\right]^2 \Delta U_{k+1}^\rho$, and

$$R_{2t}^* \equiv \sum_{i=1}^{t}\exp\left(-\frac{\phi}{T^\alpha}i - \frac{\lambda}{T^{\alpha/2}}U_i\right)\eta_i T^{\alpha/2}\sum_{k=1}^{t}\sum_{i=k+1}^{t}\exp\left(\frac{\phi}{T^\alpha}(2k-i) + \frac{\lambda}{T^{\alpha/2}}(2U_k - U_i)\right)\eta_i \Delta U_{k+1}^\rho.$$

We write the latter as $R_{2t}^* \equiv \sum_{i=1}^{t}\exp\left(-\frac{\phi}{T^\alpha}i - \frac{\lambda}{T^{\alpha/2}}U_i\right)\eta_i \times \overline{R}_{2t}^*$, in order to follow the same lines as the proof for R_t in the previous subsection. Notice that to do so, we let $T^{\alpha/2}$ appear explicitly in the definitions of R_t^*, R_{1t}^* and R_{2t}^* above, so that $\mathsf{V}\left[T^{\alpha/2}\Delta U_{k+1}^\rho\right] \to \lambda^2 \neq 0$ as $T \to \infty$. The result follows.